DOI: 10.26599/FSHW.2025.9250872

Contents lists available at SciOpen

Food Science and Human Wellness

journal homepage: https://www.sciopen.com/journal/2097-0765

China Food Publishing Co.

Hyodeoxycholic Acid and Cholesterol Sulfate as Key Modulators of Lipid Metabolism in Dyslipidemia based on Gut Microbiome and Metabolome Integrative Analysis

Kaizhang Wu [a,#], Wenqing Yu [a,#], Juncheng Liu [a], Yuwei Zhang [a], Zecheng Zhang [a], Shangwu Chen [a], Xiaoning Zhai [a], Jie Gao [a*]

[a] *School of Light Industry and Food Engineering, Guangxi University, Nanning 530004, China*

ABSTRACT: Dyslipidemia, a driver of atherosclerosis and fatty liver disease, burdens society and is associated with gut microbiota responses to dietary patterns. This study aimed to identify key intestinal metabolites involved in regulating lipid metabolism in dyslipidemia and to explore the underlying mechanisms. We performed a metabolome analysis of a humanized dyslipidemia mouse model. Then we screened out hyodeoxycholic acid (HDCA) and cholesterol sulfate (CSS) that potentially interact with farnesoid X receptor (FXR) based on molecular docking and cell culture. Oral administration demonstrated that the HDCA and CSS may ameliorate dyslipidemia via regulating bile acid metabolism, potentially mediated by activation of hepatic or intestinal FXR. Additionally, HDCA promoted the proliferation of *g_Roseburia* and *g_norank_Muribaculaceae*, and CSS enhanced the multiplication of *g_Alloprevotella*. These findings underscored that the intestinal steroid metabolites HDCA and CSS may be promising functional substances for regulating lipid metabolism.

Keywords: *Hyodeoxycholic acid, Cholesterol sulfate, Dyslipidemia, Gut microbiota*, *FXR*

1. Introduction

Dyslipidemia, a key component of metabolic syndrome, can lead to conditions such as atherosclerosis and non-alcoholic fatty liver disease (NAFLD), and its prevalence has risen in recent years, adding to the societal burden[1]. Characterized by imbalance in lipid metabolism, dyslipidemia is marked by elevated levels of total cholesterol (TC), total triglycerides (TG), and low-density lipoprotein cholesterol (LDL-C)[2]. A prospective study found a correlation between dyslipidemia and dietary patterns[3]. Gut microbiota respond to adjustments in high-fat dietary (HD) patterns as one of the causes of lipid metabolism variations[4]. Crosstalk information between dietary patterns and gut microbiota may exist key factors regulating lipid metabolism[4].

Gut microbiota, a diverse community of microorganisms inhabiting the host's gastrointestinal tract, produce a variety of metabolites that are crucial in regulating numerous physiological processes[5,6]. Primary bile acids are produced in the liver and transported through the gallbladder into the intestines where they are

# These authors contribute equally
***Corresponding author**
gaojie@gxu.edu.cn

Received 14 May 2025
Received in revised from 29 June 2025
Accepted 29 August 2025

metabolized by the gut microbiota into secondary bile acids[7]. Bile acids are natural ligands for the farnesoid X receptor (FXR), which plays a significant role in maintaining lipid metabolism homeostasis[7]. Thus, bile acids are important molecules in the regulation of lipid metabolism[8]. High dietary fibre diets supplemented with konjac glucomannan may positively affect lipid and glucose homeostasis in high-protein and carbohydrate diet mice by altering the gut microbiota and downregulating hepatic sterol regulatory element binding transcription factor 1 and FXR to reduce secondary bile acid levels[9]. Amuc protein from *Akkermansia muciniphila* reduced bile acid synthesis by activating hepatic FXR to enhance intestinal barrier function and decrease lipid deposition[10]. Our previous study demonstrated that fucogalactan sulfate from *Laminaria japonica* effectively regulated lipid metabolism by lowering bile acid synthesis and lipid absorption through the intestinal FXR-FGF15-CYP7A1/CYP8B1 pathway[11]. Another study demonstrated that activation of hepatic FXR inhibited the liver X receptor α - sterol regulatory element binding protein 1 axis to reduce hepatic cholesterol levels[12]. Diosgenin-mediated activation of peroxisome proliferator-activated receptor α by activating hepatic FXR facilitated fatty acid oxidation to alleviate NAFLD[13]. However, it remains unclear whether there are intestinal bioactive metabolites, influenced by dietary changes and shifts in gut microbiota, that interact with FXR to alleviate lipid metabolism disorders. We have previously found that fecal microbial transplantation (FMT) reshaped the gut microbiota of mice, successfully established humanized dyslipidemia model, and combined with HFD to establish diet-induced humanized dyslipidemia model[14]. The model could simulate gut microbiota in dyslipidemic populations. Dietary induction could enhance the synergistic effect between diet and gut microbiota to help capture key metabolites in the background. Therefore, humanized mouse model constructed with FMT and HD is a good strategy in the investigation of dyslipidemia gut microbiota-diet interactions.

To explore the questions above, we performed an integrated metabolome analysis of a humanized dyslipidemia mice model in an HD pattern, along with molecular docking and cell culture. Hyodeoxycholic acid (HDCA) and cholesterol sulfate (CSS) were found to be keystone bioactive steroid metabolites for potentially regulating lipid metabolism. Subsequently, oral administration revealed that HDCA and CSS mediated FXR to improve dyslipidemia.

2. Materials and methods

2.1 Chemicals

Normal diet (ND, AFF220705777) was purchased from Jiangsu Xietong Pharmaceutical Bioengineering CO., Ltd (Nanjing, China). HD (H10060) was obtained from Beijing HFK Bioscience Co., Ltd (Beijing, China). Formic acid and methanol of LCMS grade were supplied by Thermo-fisher Scientific (Waltham, MA, USA). CSS (> 98%), quinestrol (QET, > 98%), sarsasapogenin (SAR, > 98%), and HDCA (> 98%) was purchased from Shanghai Macklin Biochemical Co., Ltd (Shanghai, China). The composition of ND and HD are shown in Table S1.

2.2 Animal Studies

FMT solution was produced as in previous study[14]. Briefly, healthy individuals and patients with dyslipidemia from Guangxi University Hospital and Fourth People's Hospital of Nanning were recruited as donors. The approximate 2 g fresh fecal sample from dyslipidemia donors was placed in 20 mL of sterile saline solution (0.9%, w/v) and immediately sealed with liquid paraffin. Samples were rapidly transported to an anaerobic workstation (HYQX-III-Z, Shanghai Yuejin Medical Instrument Co., Ltd., Shanghai, China). The stool sample mixtures were filtered using sterile gauze in in an anaerobic environment (5% H_2, 5% CO_2, and 90% N_2). The filtrate was diluted and formed FMT solutions (from healthy individuals, Table S2) and hyperlipidemia fecal microbial transplants (HFMT) solutions (from patients with dyslipidemia individuals, Table S2). C57BL/6J mice (SPF, male, aged 3-4 weeks) were obtained from Si Pei Fu Biotechnology Co., Ltd. (Beijing, China) and were free to access purified water and ND for a two-week acclimatization period. Animals were housed in individually ventilated cages under a controlled environment (12 h light-dark cycle at room temperature 20-25 ℃ and relative humidity at 30%–70%). At the end of the experiment, all of the mice were humanely euthanized. Liver and blood samples were collected for further study[11,15]. The study had passed the animal experiment ethics review of the Medical Ethics Committee of Guangxi University (Approval No.: GXU-20230035).

2.2.1 Animal Experiment 1

The C57BL/6J mice were randomly divided into 4 groups (n = 6 per group). To explore the effects of human-derived gut microbiota on lipid metabolism in mice, after the acclimation period, all mice were intragastrically administered with 10 mL/kg fresh composite antibiotics (1 g/L of neomycin sulfate, 1 g/L of metronidazole, 1 g/L of ampicillin, and 0.5 g/L of vancomycin, Abbreviations: AT) each day for two weeks. After the antibiotic treatment, two groups were orally gavaged with FMT solution (10 mL/kg/day) and were separately fed ND and HD for 8 weeks (named FMT+ND and FMT+HD groups). The other two groups were gavaged daily with HFMT solution (10mL/kg/day) and were fed ND and HD, respectively, for 8 weeks (named HFMT+ND and HFMT+HD groups). All mice were treated with 0.9% NaCl during 2 weeks of recovery.

2.2.2 Animal Experiment 2

For investigating the effects of HDCA and CSS on dyslipidemia mice, the C57BL/6J mice were randomly divided into 4 groups (NC, MC, HDCA, and CSS, n = 6 per group). After oral treatment with fresh composite antibiotics for 2 weeks, the NC group was treated with FMT and the other three groups of mice were treated with HFMT solution for 8 weeks. After 2 weeks of recovery, HDCA and CSS groups were separately gavaged with HDCA and CSS (100mg/kg/day, corn oil as solvent) during the next 4 weeks. NC and MC groups were treated with corn oil at the same time.

2.3 Biochemical Analysis

Automatic Biochemical Analyzer (ZY-1280, Kehua Bio-Engineering Co., Ltd, Shanghai, China) were used to detect the serum concentrations of TC, TG, high-density lipoprotein cholesterol (HDL-C), LDL-C, aspartate aminotransferase (AST), and alanine aminotransferase (ALT).

2.4 Hematoxylin and Eosin (H&E) and Immunofluorescence Staining

The liver and colon tissues of mice were fixed in 4% paraformaldehyde and embedded in paraffin. The sections were stained with H&E. Finally, the sections were sealed with neutral gum and observed with a microscope. The immunofluorescence staining was performed according to previous study[16]. The liver and colon sections were exposed to the primary antibodies (rabbit anti-FXR polyclonal antibody and rabbit anti-CYP7A1 antibody) at 4 ℃ overnight. After incubation, the sections were washed three times with PBS and incubated with biotinylated Cy3-conjugated Affinipure Goat Anti-Rabbit IgG (H + L). The nuclei were counterstained with 4',6-diamidino-2-phenylindole. Finally, microscopic imaging was performed using a Zeiss Imager.Z2 fluorescence microscope.

2.5 Gut Microbiota Analysis

DNA was obtained from feces using the E.Z.N.A™ Mag-Bind Stool DNA Kit (Cat: M5635-02, OMEGA, USA) with confirmed DNA isolation via agarose gels based on the manufacturer's instructions. Polymerase chain reaction (PCR) amplicons were created from the target region V3-V4, using 314F (CCTACGGGNGGCWGCAG) and 805R (GACTACHVGGGTATCTAATCC). DNA sequencing and analysis were conducted on an Illumina MiSeq system (Illumina MiSeq, USA). Finally, all paired-end reads were merged into operational taxonomic units (OTUs). OTUs were classified taxonomically by blasting against the RDP Database.

2.6 Untargeted Metabolome Analysis

Metabolome analysis of feces was performed with Q Exactive Plus system (Thermo-fisher Scientific, MA, USA). 50 mg sample was added to 600 μL of methanol and vortexed for 60 s. Then, the mixture was centrifuged and the supernatant was obtained. Ultra performance liquid chromatography-mass spectrometry/mass spectrometry (UPLC-MS/MS) equipped with Hypersil GOLD C18 column (100 mm × 2.1 mm, 1.9 um. Thermo-fisher Scientific) and mobile phase of 0.1% formic acid and methanol were used. Electrospray ionization (ESI) was used for metabolite detection at 3.0 kV in switching mode. The data were collected according to the range (100 to 1000 m/z) under a resolution of 70,000 FWHM. For dd-MS^2, the mass spectra were recorded at a resolution of 17500 FWHM. Fragment ions were generated in HCD collision cells using stepped normalized collision energy (NCE 10, 25, and 45%). Compound Discoverer software (Thermo Scientific, Waltham, MA, USA) was performed to analyze the results.

2.7 Targeted Metabolome Analysis.

Feces were reconstituted in methanol. After being vortex-mixed vigorously, the samples were centrifuged to remove precipitates at 4 ℃ for 15 min with a speed of 12,000 × g. Chromatographic separation was performed on a Shim-pack GIS C18 column. Mobile phase A was 0.1% formic acid and mobile phase B

was methanol. The ESI source conditions were set as follows: ion source gas1, 50; ion source gas2, 50; curtain gas, 35; source temperature, 500 ℃; IonSpray voltage floating, -4500 V. The data were collected according to the 100-1000 Da m/z range. Mass data acquisition was performed using an AB X500R (SCIEX, Framingham, MA, USA) in multiple reaction monitoring (MRM) mode to monitor bile acids at m/z range of 50-600 Da. MRM conditions were shown in Table S3.

2.8 Real-time Quantitative PCR (RT-qPCR)

The total mRNA was extracted using the classical Trizol method. The cDNA was synthesized through the BeyoRT Q First Strand cDNA Synthesis Kit. The quantitative PCR was performed with LightCycler 96 system (Roche, Basel, Switzerland). The mRNA levels were normalized with GAPDH as a housekeeping gene. The primer sequence in the qPCR analysis were shown in Table S4.

2.9 Molecular Docking

To explore the interaction between the metabolite and the receptor FXR, we employed the AutoDock Vina (version 1.1.2) to perform molecular docking. The metabolite 2D structure were obtained from the PubChem database (https://pubchem.ncbi.nlm.nih.gov). The 3D structures of metabolites were drawn using KingDraw V5.0. The 3D structural model of the FXR（PDB ID: 1OSH） was obtained from the RCSB PDB database (https://www. rcsb. org). The docking active site of FXR was set to (17.7, -14.3, -39.2). We established 3D affinity grid (20 Å × 16 Å × 20 Å) with a spatial interval of 0.375 Å between grid points. The resulting docking data were processed and analyzed using PyMOL (version 2.0) software and Discovery Studio (version 21.1.0.20298) software.

2.10 Cell Culture and CCK-8 Assay

Caco-2 cells were cultivated in Dulbecco's Modified Eagle Medium containing 10% fetal bovine serum, 1% penicillin/streptomycin, and 1% non-essential amino acids under an atmosphere of 5% CO_2 at 37 ℃. For cytotoxicity analysis, Caco-2 cells (5×10^4 cells/well) were seeded into 96-well plates, preincubated for 24 h and then treated with 0%, 0.1%, and 1% dimethyl sulfoxide (DMSO). Additionally, Caco-2 cells were treated with HDCA, CSS, QET, and SAR (5, 10, 25, 50, 100, 250, and 500 μmol/L, 0.1% DMSO as cosolvent). Cell viability was determined using the CCK-8 assay and measured with a Microplate Reader Infinite 200 pro (TECAN, Männedorf, Switzerland) at 490 nm.

2.11 Effect Evaluation of Metabolites on FXR

Caco-2 cells were seeded into 96-wellplates at a density of 5×10^4 cells/mL and cultured overnight. Then, the cells were cultured with 100 μmol/L HDCA, CSS, QET, and SAR for 24 h. The supernatant was removed, and the mRNA were analyzed according to the method of 2.8.

2.12 Statistical Analysis

The experimental results were expressed as mean ± standard deviation (SD). Student t-test and one-way analysis of variance (ANOVA) were performed using IBM SPSS statistics (Version 26.0). Multiple

comparisons among groups were performed using Tukey test. Statistical significance was established at a level of $P < 0.05$. GraphPad Prism 8.0 and R package were used for the graphic presentation.

3. Results

3.1 HDCA was Negatively Associated with Dyslipidemia.

To discern bioactive metabolites from the interaction between HD and dyslipidemia gut microbiota, we investigated metabolite profiles by establishing a dyslipidemia mice model in HD pattern via FMT (Figure 1a). TC, TG, HDL-C, and LDL-C significantly increased through HD ($P < 0.05$) (Figure 1b). Blood lipids were elevated further by the HFMT treatment (Figure 1b). H&E staining indicated liver swelling and blistering by HD (Figure 1c). Meanwhile, accumulation of hepatic lipid droplets was indicated in HD with Oil Red O staining, especially more apparent in mice with HFMT (Figure 1c).

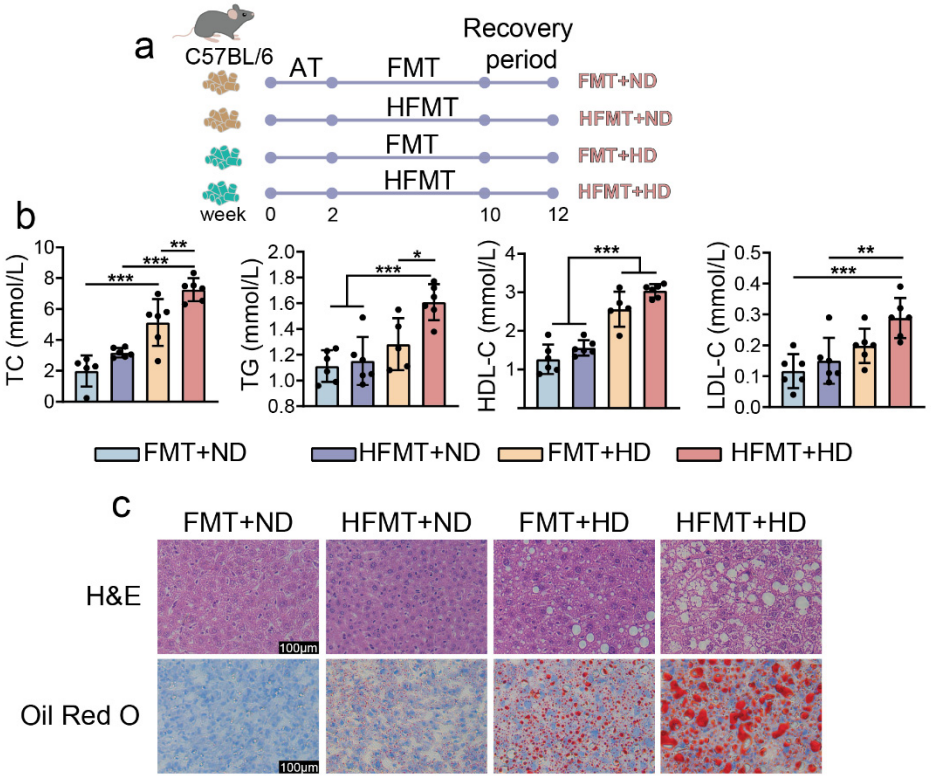

Figure 1. HFMT induced dyslipidemia in mice, and promoted phenotypes in HD pattern. (a) Illustration of FMT and HFMT treatment experiment. (b) Serum TC, TG, HDL-C, and LDL-C. (c) H&E and Oil Red stained liver samples. Data were shown as mean ± SD. The *p* values were determined by one-way ANOVA using Tukey test. *$P < 0.05$, **$P < 0.01$, ***$P < 0.001$.

Principal coordinate analysis (PCoA) with 16S rRNA high-throughput sequencing showed that HD and HFMT altered the structure of gut microbiota (Figure S2a). A key contribution of gut microbiota changes to host physiology is to cause changes in their derived metabolites[17]. We next evaluated metabolic profiling changes in mice after modeling. The fecal metabolites of mice were annotated and analyzed. Metabolites were divided into eight categories, which were lipids, amino acids, peptides, nucleotides, carbohydrates, cofactors and vitamins, xenobiotics, and biosynthesis of other secondary metabolites. Metabolite differences were compared between the HFMT+ND and FMT+ND groups, as well as between the HFMT+HD and FMT+HD groups, according to $\log_2$(Fold Change). The metabolites with the highest number of |$\log_2$(Fold

Change)|>1 were all lipids after HFMT treatment in ND and HD patterns (Figure 2a). Differential metabolites were screened with the criteria of $P < 0.05$ and $|\log_2(\text{Fold Change})| > 1$. Under the ND pattern, 127 metabolites were considerably upregulated, while 164 metabolites were notably downregulated in the HFMT+ND group compared to the FMT+ND group (Figure 2b). In contrast, under the HD pattern, 36 metabolites were markedly upregulated and 39 metabolites were significantly downregulated in the HFMT+HD group compared to the FMT+HD group (Figure 2b). We found that HD could reduce the differences in lipid metabolites for HFMT in mice. We screened for steroid metabolites from the differential metabolites. 9 differential steroid metabolites were screened between HFMT and FMT under the HD, which was less than the 64 kinds under the ND. (Figure 2c). Hence, HD may reduce the discrepancy in lipid metabolites in mice affected by HFMT.

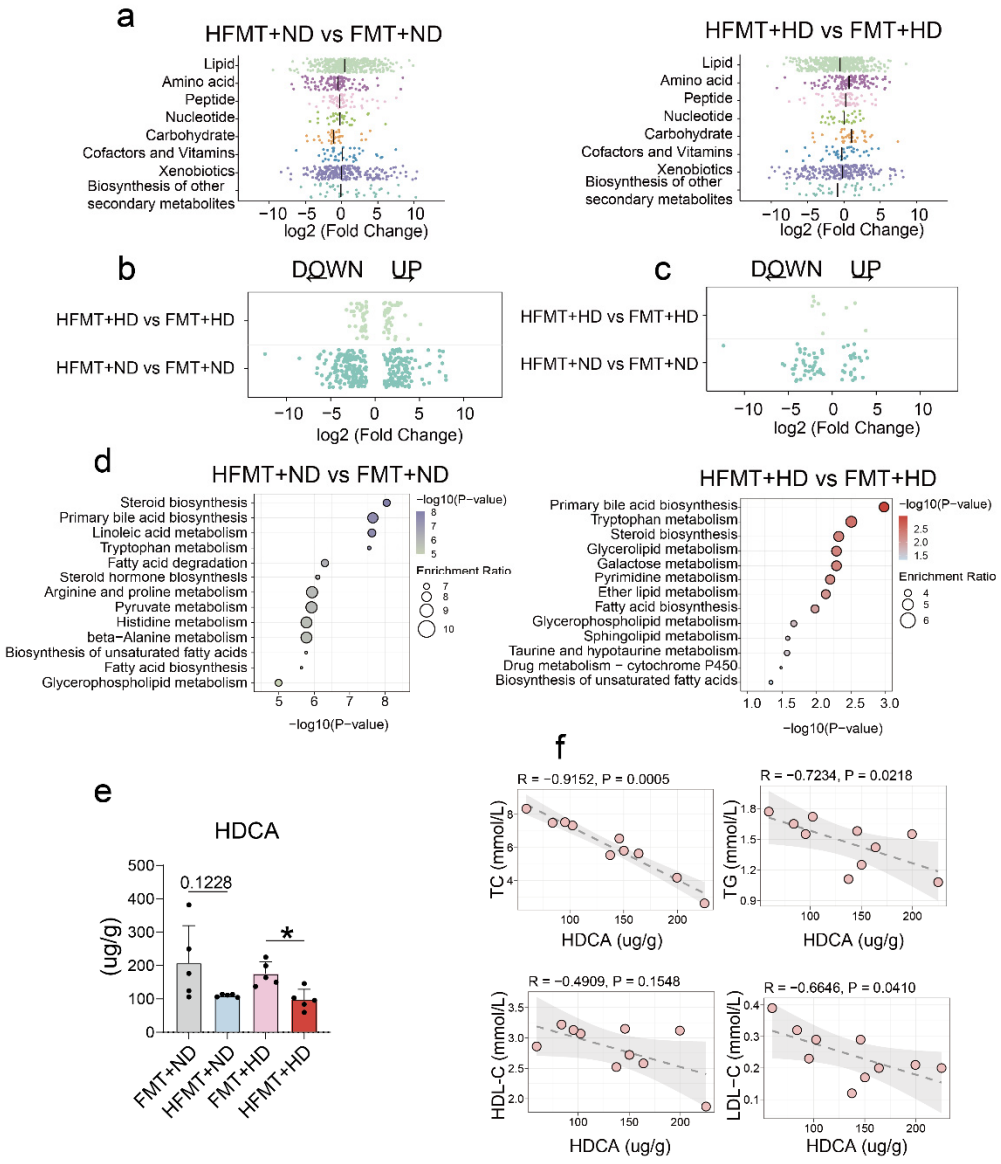

Figure 2. HDCA inversely correlated with the risk of dyslipidemia. (a) Differential metabolite annotation in HFMT+ND versus FMT+ND and HFMT+HD versus FMT+HD. (b) The Fold Change of differential metabolites in HFMT versus FMT under ND and HD. (c) The Fold Change of differential steroid metabolites in HFMT versus FMT under ND and HD. (d) KEGG pathway enrichment analysis of the differential metabolites in HFMT versus FMT under ND and HD. (e) HDCA level in fecal samples. (f) Correlations between HDCA and TC, TG, LDL-C, and HDL-C. Data were shown as mean ± SD. The *p* values were determined by one-way ANOVA using Tukey test. *$P < 0.05$.

Enrichment analysis revealed that HFMT could induce significant alterations in lipid metabolism based on the Kyoto Encyclopedia of Genes and Genomes (KEGG) databases, such as Steroid biosynthesis, Primary bile acid biosynthesis, Fatty acid degradation, Steroid hormone biosynthesis, Biosynthesis of unsaturated fatty acids, Fatty acid biosynthesis, and Glycerophospholipid metabolism (Figure 2d). In addition, Primary bile acid biosynthesis was the most significantly changed metabolic pathway in the HD pattern (Figure 2d). To further analyze the metabolites in the pathway, the quantification of bile acid was performed by UPLC-MS/MS (Figure S2b). HDCA was downregulated by HFMT, and the HDCA downregulation could be enhanced dramatically by HD ($P < 0.05$, Figure 2e). Furthermore, correlation analysis demonstrated that HDCA was negatively correlated with TC, TG, and LDL-C ($P < 0.05$, Figure 2f). Therefore, HDCA was negatively associated with increased risk of dyslipidemia.

3.2 HDCA and CSS May be the Key Metabolites interacting with FXR.

In addition to HDCA, we were also interested in whether other non-bile acid steroid metabolites are bioactive metabolites related to dyslipidemia. We extracted compounds from differential steroid metabolites for subsequent analysis (Figure 2c). Molecular docking can assist in understanding structure-activity relationships between proteins and small molecules as a bioinformatics tool[18]. To explore the role underlying HDCA and the non-bile acid steroid metabolites on FXR, we performed 50 molecular dockings to analyze the binding energy between metabolites and FXR protein. The top 10 steroid metabolites that displayed well bound affinities (affinity < -6 kcal/mol) with the lowest binding energy were selected (Table 1). CSS (-12.76 ± 0.40) kcal/mol, QET (-12.33 ± 1.03) kcal/mol, and SAR (-11.93 ± 0.02) kcal/mol, three metabolites with the lowest binding energy, were selected from the top 10 metabolites for further analysis according to the purchasable and obtainable of the compound. Additionally, the binding energy of HDCA to FXR was (-10.56 ± 0.48) kcal/mol. According to the docking results, the active site interactions of HDCA, CSS, QET, and SAR were mainly controlled by hydrophobic interaction, such as Pi-Alkyl, Alkyl, and Pi-Sigma (Figure 3a).

Table 1. The binding energy between differential metabolites and FXR protein.

Metabolites	Pubchem ID	Binding energy (kcal/mol)
Cholesterol sulfate	65076	-12.76 ± 0.40
4,4-Dimethyl-5α-cholesta-8,14,24-trien-3β-ol	443212	-12.34 ± 1.50
Quinestrol	9046	-12.33 ± 1.03
Crinosterol	5283660	-12.24±0.50
17-Hydroxypregnenolone sulfate	152971	-12.13 ± 2.00
Zymosterol	92746	-11.93 ± 0.55
Sarsasapogenin	92095	-11.93 ± 0.02
Solanidine	65727	-11.87 ± 0.02
4,4-Dimethyl-5a-cholesta-8,24-dien-3-b-ol	50990081	-11.78 ± 0.46
7alpha-Hydroxy-4-cholesten-3-one	123743	-11.60 ± 0.58

To evaluate the cytotoxicity of DMSO (metabolite latent solvent) and metabolites, the viability of Caco-2 cells was determined at different concentrations of the DMSO and metabolites. Cell viability assay suggested that 0.1% DMSO had hardly any effect on cells (Figure 3b). At metabolite concentrations above 100 μM, cell viability in HDCA, QET, and SAR were decreased to less than 80%, whereas Caco-2 cells

were able to tolerate high CSS concentrations (Figure 3c). Next, 100 μM was selected as intervention concentration of cell culture. The active effects of CSS on cells can be significantly observed in qPCR results ($P < 0.05$, Figure 3d). Moreover, HDCA had a small activated effect on FXR ($p = 0.056$, Figure 3d). Taken together, FXR in cells could be affected by HDCA and CSS. However, due to the difficulty in constructing metabolic models in cells, the actual effects of HDCA and CSS in FXR need further *in vivo* trial verification.

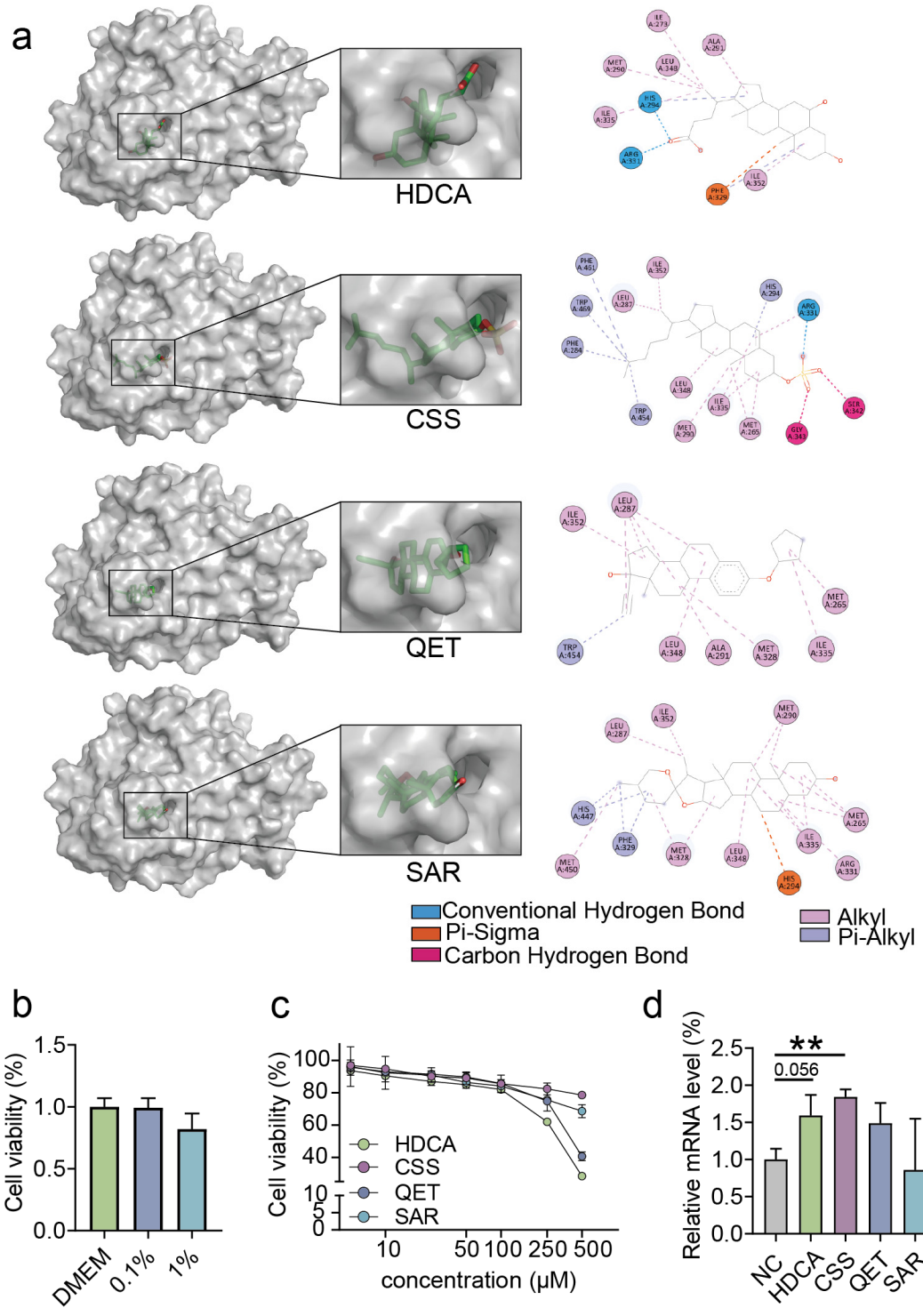

Figure 3. HDCA and CSS may interact with FXR. (a) Docking interactions of HDCA, CSS, QET, and SAR with FXR. (b) Toxicity evaluation of DMSO for Caco-2 cell. (c) Toxicity evaluation of HDCA, CSS, QET, and SAR for Caco-2 cell. (d) Relative mRNA expression of FXR treated with HDCA, CSS, QET, and SAR. Data were shown as mean ± SD. The *p* values were determined by one-way ANOVA using Tukey test. *$P < 0.05$, **$P < 0.01$.

3.3 Oral Supplementation with HDCA and CSS Ameliorated Dyslipidemia in mice.

To examine the protective effects of HDCA and CSS on dyslipidemia, HDCA and CSS supplementation were performed in a humanized dyslipidemia mice model based on our previous approach[14] (Figure 4a). Levels of serum TC, TG, LDL-C, and ALT in the HDCA and CSS groups were markedly lower than those in the MC group ($P < 0.05$, Figure 4b). In the HDCA group, serum AST levels showed a significant reduction ($P < 0.05$, Figure 4b). Furthermore, by H&E and oil red O staining, reduced hepatic vacuoles and lipid droplets were observed in the HDCA and CSS groups compared to MC group (Figure 4c).

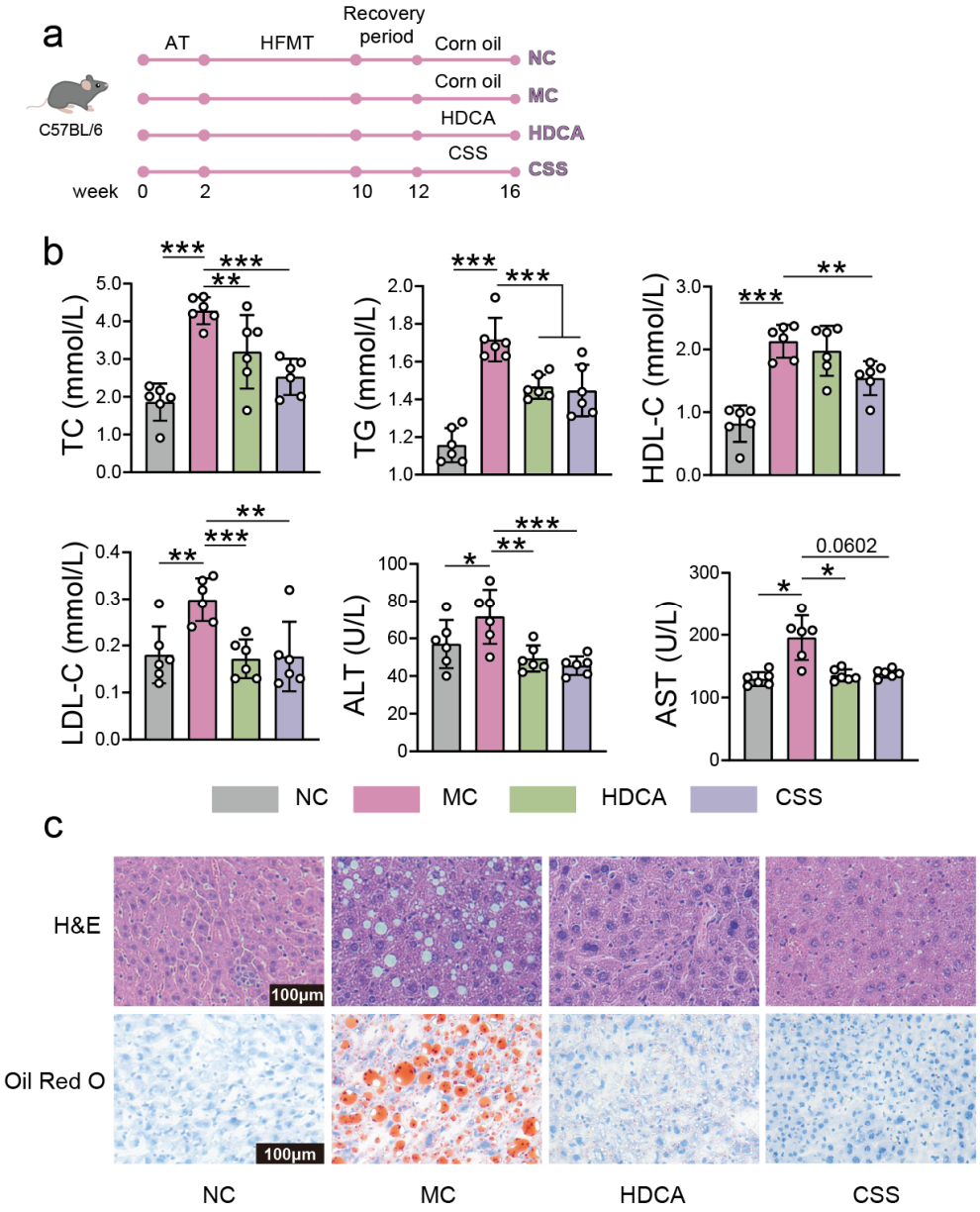

Figure 4. HDCA and CSS supplementation ameliorated dyslipidemia in mice. (a) Illustration of HDCA and CSS treatment experiment. (b) Serum TC, TG, HDL-C, LDL-C, ALT, and AST. (c) H&E and Oil Red stained liver samples. Data were shown as mean ± SD. The *p* values were determined by one-way ANOVA using Tukey test. *$P < 0.05$, **$P < 0.01$, ***$P < 0.001$.

We also investigated the gut microbiota response to HDCA and CSS interventions via 16S high-throughput sequencing. PCoA based on Bray-Curtis distance showed significant differences among gut

microbiota of groups (Figure 5a). HDCA and CSS had some recovery effect on HD-induced Simpson and Shannon indexes reduction(Figure 5b). The relative abundance of *g_Eubacterium_fissicatena_group* was downregulated by HDCA and CSS (Figure 5c-d). In addition, HDCA and CSS treatments were successful in improving relative abundance of some genus, including *g_norank_Muribaculaceae*, *g_norank_Oscillospiraceae*, and *g_unclassified_Lachnospiraceae* (Figure 5c-d). Meanwhile, HDCA elevated the relative abundance level of *g_Alistipes*, *g_Roseburia*, *g_norank_Ruminococcaceae*, *g_Intestinimonas*, and *g_Anaerotruncus* compared to the MC group (Figure 5c-d). Furthermore, Linear discriminant analysis Effect Size (LEfSe) analysis discovered that *g_Alloprevotella* and *g_norank_Clostridia_vadinBB60_group* were increased after CSS treatment versus the MC group (Figure 5d).

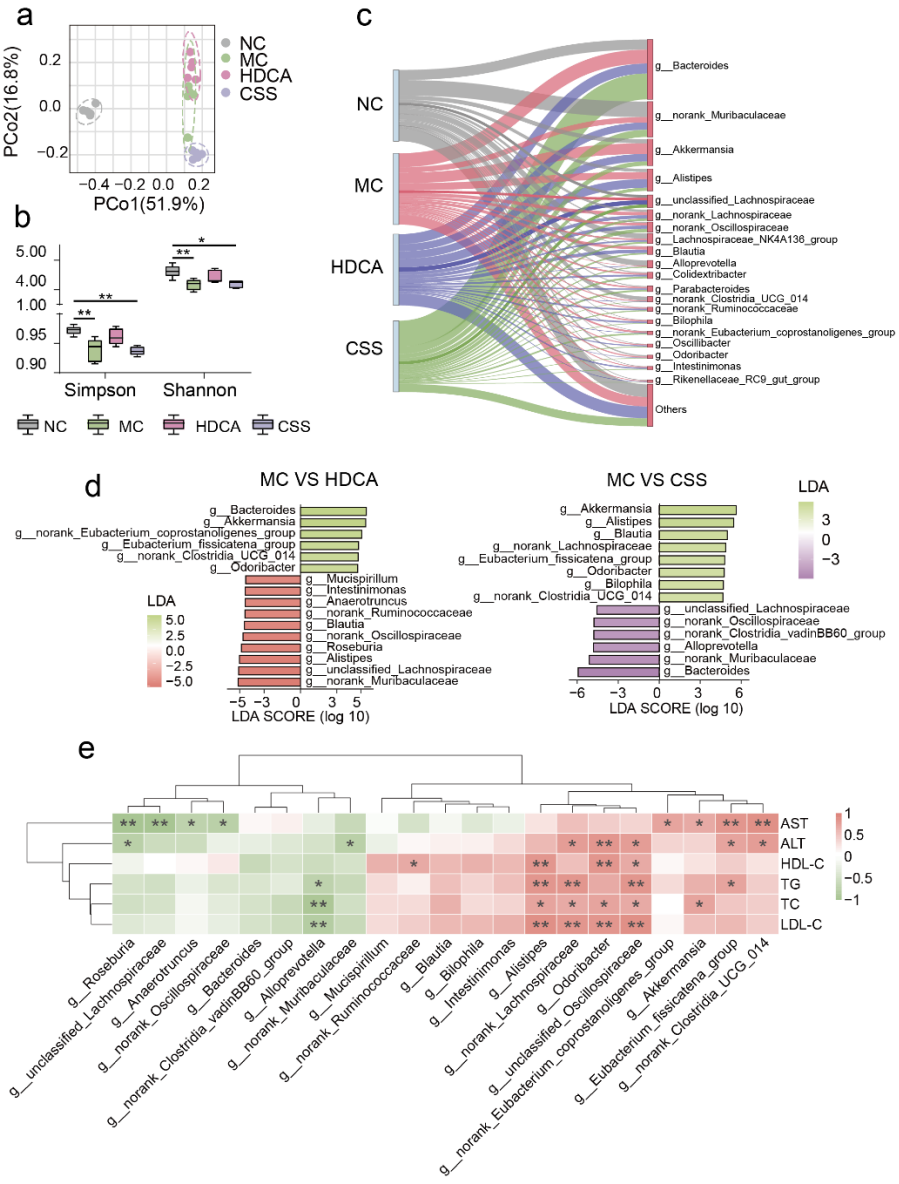

Figure 5. HDCA and CSS modulated the structure of gut microbiota. (a) PCoA based on Bray-Curtis distance. (b) Simpson and Shannon indexes. (c) Relative abundance at genus level of gut microbiota. (d) LEfSe plots to show the characteristic gut microbiota of MC versus HDCA and MC versus CSS (LDA > 4.5). (e) Heatmap of Spearman's correlation between lipids-related clinical indicators and gut microbiota at genus level. Red indicated positive correlation, and green indicated negative correlation. Data were expressed as mean ± SD. Differences of data were calculated by the one-way ANOVA using Tukey test. *$P < 0.05$; ** $P < 0.01$.

In order to assess the association of gut microbiota with physiological phenomenon, spearman's correlation analysis was performed between differential gut microbiota and biochemical indexes among the intervention and MC groups. The relative abundance of *g_Alistipes*, *g_norank_Lachnospiraceae*, and *g_unclassified_Oscillospiraceae* were significantly positively associated with TC, TG, and LDL-C (P < 0.05, Figure 5e). Notably, the relative abundance of *g_Roseburia* was negatively correlated with AST and ALT (P < 0.05, Figure 5e). g_*Eubacterium_fissicatena_group* and *g_norank_Eubacterium_coprostanoligenes_group* were positively associated with AST and ALT (P < 0.05, Figure 5e). On the contrary, TC, TG, and LDL-C were negatively correlated with the relative abundance of *g_Alloprevotella* (P < 0.05, Figure 5e). Of note, *g__Romboutsia*, *g_unclassified_Lachnospiraceae*, *g_Anaerotruncus*, and *g_norank_Oscillospiraceae* were negatively associated with AST (P < 0.05, Figure 5e). In brief, HDCA and CSS ameliorated dyslipidemia induced by HFMT and HD. At the same time, the structure of gut microbiota might be modulated by HDCA and CSS.

3.4 Supplementation with HDCA and CSS Resulted in Broad Changes in Fecal Metabolome and Highlighted Changes in Bile Acid Metabolism.

To fully characterize the impact of HDCA and CSS on fecal metabolites, untargeted metabolome analysis of fecal samples was performed using UPLC-MS/MS. Compared with MC group, the principal components analysis (PCA) score plot showed that administration of HDCA and CSS could significantly alter the metabolic profiles of mice (Figure S3a). Clear variations were demonstrated after oral intake of HDCA and CSS based on the Orthogonal partial least squares-discriminant analysis (OPLS-DA) (Figure S3b-c). According to the thresholds of P < 0.05 and $|\log_2(\text{Fold Change})| > 1$, the volcano plot exhibited that the 80 metabolites showed upregulation while 126 metabolites were downregulated in the HDCA group compared to the ND (Figure 6a). Consistently, differences were found between the CSS and MC groups, including 94 upregulated and 285 downregulated metabolites (Figure 6a). Pathway enrichment analysis revealed that Primary bile acid biosynthesis was the significant metabolic pathway after HDCA and CSS treatments based on KEGG database (Figure 6b). Therefore, targeted metabolome analysis for bile acids was performed to investigate changes in fecal bile acid profile by HDCA and CSS. HDCA and its conjugated forms taurohyodeoxycholic acid (THDCA) and glycohyodeoxycholic acid (GHDCA) were significantly elevated after HDCA supplementation (P < 0.05, Figure 6c). Chenodeoxycholic acid (CDCA) was dramatically elevated and taurochenodeoxycholic acid **(**TCDCA) also tended to be elevated in the HDCA group (Figure 6c). UDCA and TUDCA had an increasing trend in the HDCA group (Figure 6c). Moreover, LCA and Deoxycholic acid **(**DCA) were notably promoted after CSS treatment (P < 0.05, Figure 6c). Reduced level of primary bile acids was observed in the CSS group, and secondary bile acid levels were elevated by HDCA and CSS (P < 0.05, Figure 6c). Additionally, spearman's correlation showed that *g_Alistipes* was positively correlated with Glycocholic acid (GCA) and Taurocholic acid (TCA) (P < 0.05, Figure 6d). UDCA was positively correlated with *g_unclassified_Lachnospiraceae*, *g_Blautia*, *g__Alloprevotella*, *and g_Anaerotruncus* (P < 0.05, Figure 6d). Deoxycholic acid (DCA) and LCA were

positively associated with *g_unclassified_Lachnospiraceae* ($P < 0.05$, Figure 6d). Negative correlations were observed between HDCA and *g_norank_Clostridia_UCG_014*, and *g_Odoribacter* ($P < 0.05$, Figure 6d). Positive correlations were observed between HDCA and *g_unclassified_Lachnospiraceae*, *g_Roseburia*, *g_Blautia, g__norank_Oscillospiraceae*, and *g_Anaerotruncus* ($P < 0.05$, Figure 6d). Collectively, these results revealed that HDCA and CSS may modulate bile acid metabolism in mice.

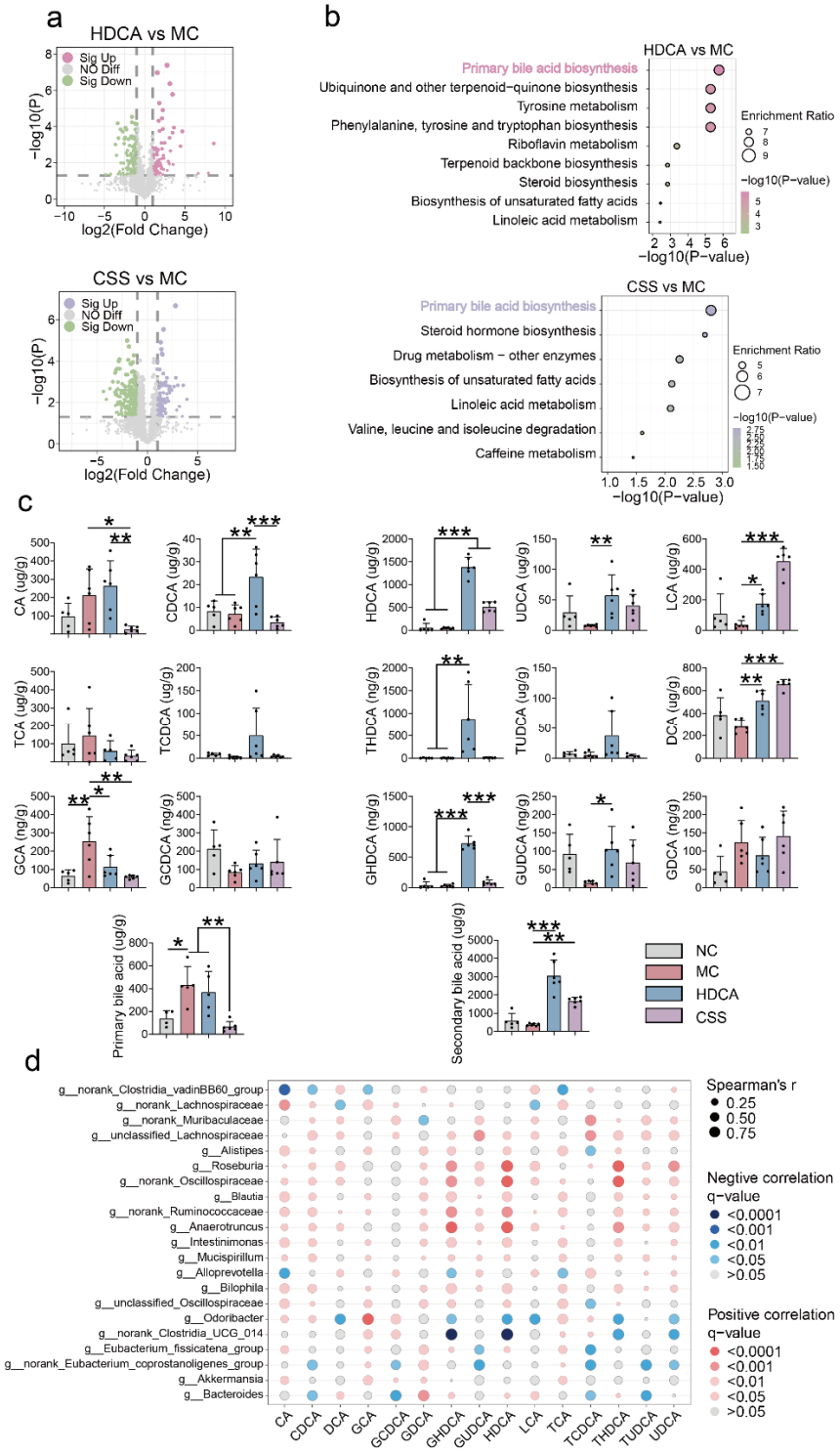

Figure 6. Bile acid metabolism was significantly altered by HDCA and CSS. (a) Volcano plots of differential metabolites in mice treated with HDCA and CSS compared with MC. (b) KEGG pathway enrichment analysis of the differential metabolites after HDCA and CSS treatments. (c) Bile acid profile in fecal samples. (d) Bubble Chart of Spearman's correlation between bile acids and differential genera. Bubble size indicated degree of relevance, red indicated positive correlation, and blue indicated negative correlation. Data were expressed as mean ± SD. Differences of data were calculated by the one-way ANOVA using Tukey test. *$P < 0.05$; ** $P < 0.01$.

3.5 HDCA and CSS Modulated Bile Acid Production.

We further conducted a signaling pathway analysis of mice treated with different interventions to investigate lipid-reducing mechanisms. RT-qPCR analysis revealed that hepatic CYP7A1 and CYP8B1 were significantly downregulated by HDCA and CSS ($P < 0.05$, Figure 7a). Hepatic FXR tended to be upregulated in the HDCA group, and hepatic SHP was notably enhanced after HDCA treatment ($P < 0.05$, Figure 7a). In addition, intestinal FXR and FGF15 were remarkably elevated by CSS ($P < 0.05$, Figure 7a). The immunofluorescence results of CYP7A1, CYP8B1, and intestinal FXR were consistent with the relative expression results of the gene (Figure 7b). Western blot analysis showed that hepatic FXR was activated in HDCA group (Figure 7c). Hepatic fibroblast growth factor receptor 4 (FGFR4) protein expression was upregulated after CSS intervention (Figure 7c). These results suggested that HDCA and CSS may mediate FXR to regulate bile acid metabolism.

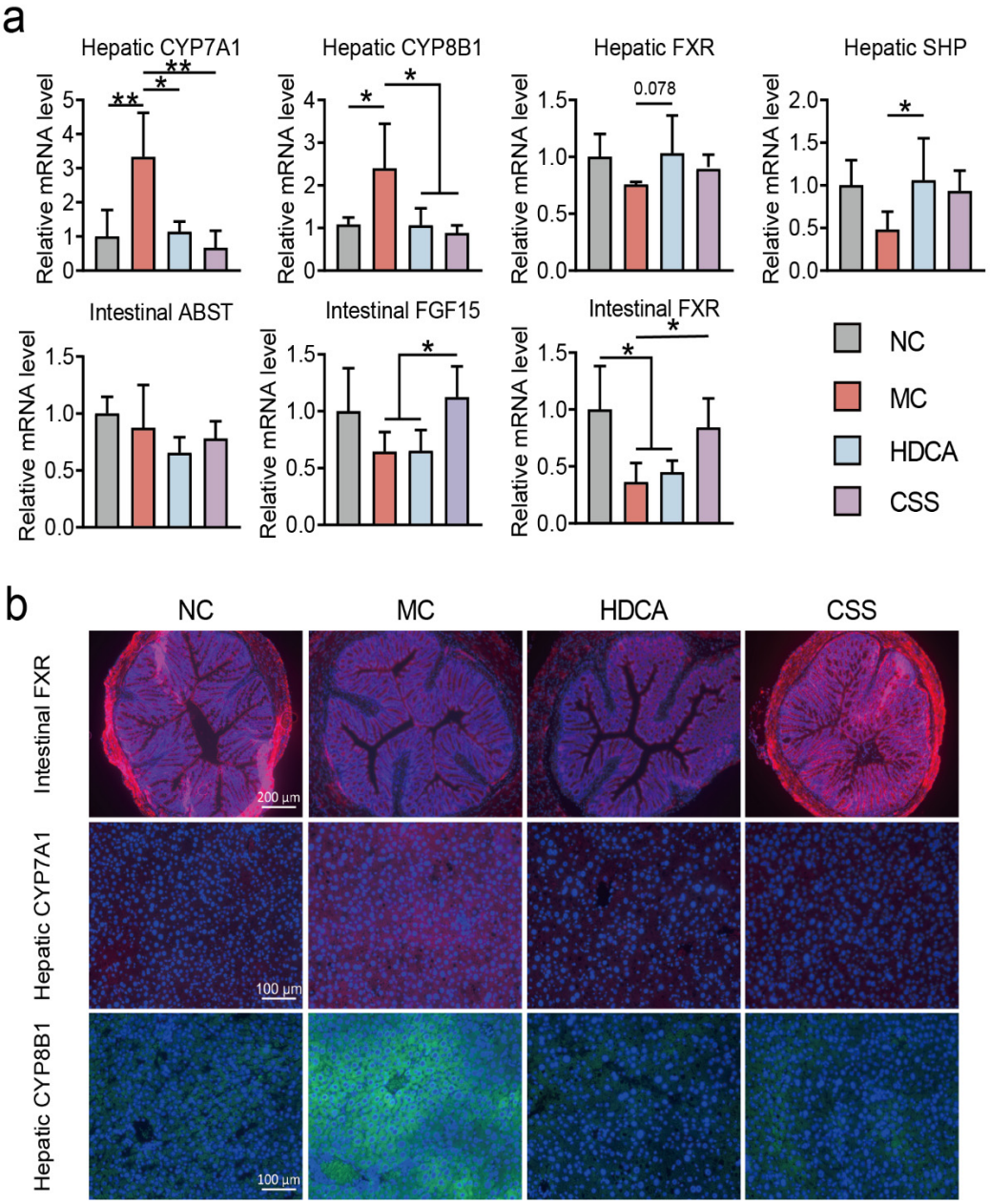

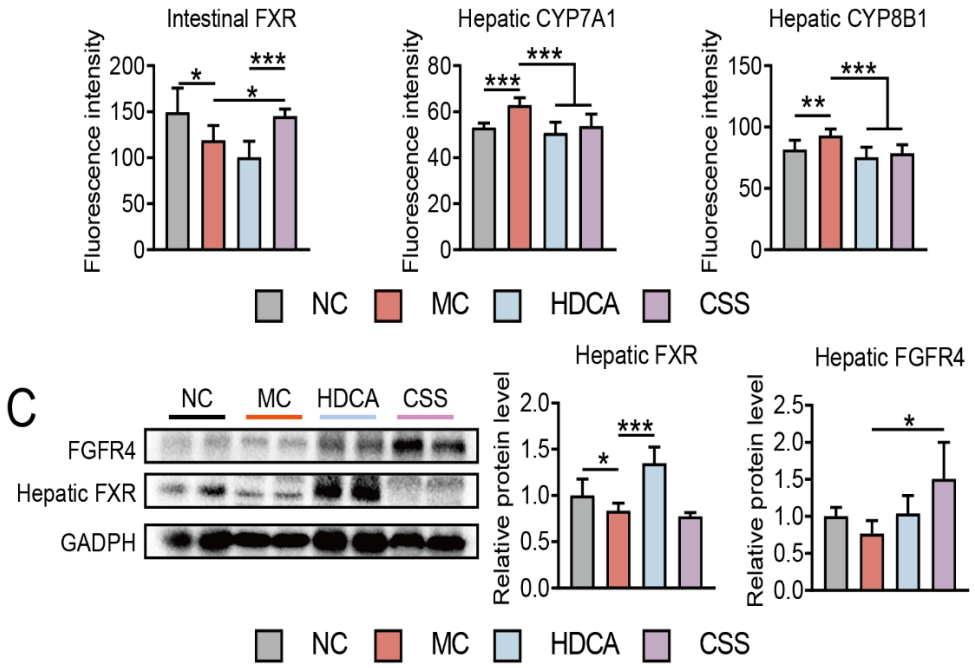

Figure 7. HDCA and CSS regulate bile acid metabolism by mediating FXR. (a) Relative mRNA level in liver and intestine. (b) Immunofluorescence analysis of hepatic CYP8B1, CYP7A1, and intestinal FXR. (c) Western blot analysis of FGFR4 and FXR protein in the liver.

4. Discussion

Dyslipidemia is a risk factor for NAFLD and is usually associated with unhealthy dietary habits, such as high-fat diet[19]. The gut microbiota plays a crucial role in host metabolism by producing bioactive metabolites, and recent researches have linked dyslipidemia-associated gut microbiota to disruptions in lipid metabolism[1,17,20]. Metabolome was used to provide an interpretation of human physiology in the context of disease[21]. Identifying bioactive metabolites effective in regulating lipid metabolism from the metabolome is meaningful. To enhance the crosstalk between dyslipidemia-associated gut microbiota and HD to discover bioactive metabolites, we performed humanized dyslipidemia mice modeling. Our results showed that primary bile acid synthesis was the most significantly altered pathway in lipid metabolism. Primary bile acids produced by the liver are transported to the gut where they are transformed into secondary bile acids by the gut microbiota, and about 95% of these bile acids are reabsorbed back to the liver via the portal vein at the terminal section of the ileum that is known as the enterohepatic circulation[7]. Bile acids are key regulators of lipid metabolism, some of which are endogenous ligands for FXR and regulate lipid metabolism, such as Lithocholic acid (LCA), Ursodeoxycholic acid (UDCA), and Tauroursodeoxycholic acid (TUDCA)[22-24]. Fecal HDCA level was significantly negatively correlated with lipid parameters (TC, TG, and LDL-C) according to correlation analysis. Therefore, dyslipidemia induced by gut microbiota and HD may be associated with dysregulation of HDCA.

Bile acids are natural steroid metabolites that are involved in the regulation of lipid metabolism[25]. Natural steroids and their derivatives possess a diverse array of biological functions[26]. Molecular docking analysis indicated that HDCA has the potential to interact with FXR. The question of whether other steroid

metabolites are involved in the FXR-mediated regulation of lipid metabolism made us consider. Hence, the remaining steroid metabolites were subjected to molecular docking with FXR for analysis. HDCA and three steroid metabolites (CSS, QET, SAR) with the lowest affinity for the FXR were selected for cell experiments. Consistent with a previous study, HDCA exerted a weak activating effect on FXR[27]. The observed increase in FXR mRNA expression indicated that HDCA and CSS may be involved in regulating the lipid metabolism within the organism via activating FXR. Nevertheless, bioinformatics-based molecular docking and cell experiments may not fully capture *in vivo* complexities.

Following the FMT modeling, we conducted oral interventions with HDCA and CSS, which confirmed their role in alleviating dyslipidemia and hepatic lipid accumulation. Notably, the abundance of *g_Eubacterium_fissicatena_group* and *g_norank_Clostridia_UCG_014* (characteristic bacteria of lipid metabolism disorder) were dramatically reduced by HDCA and CSS[28]. In addition, *g_norank_Muribaculaceae* was increased by HDCA. Several studies have reported that *g_norank_Muribaculaceae* was associated with the conversion of cholesterol to CA[29,30]. It may explain the observed increase in CA following HDCA treatment. Similarly, the abundance of *g_Roseburia* was elevated after HDCA treatment. A study investigating the regulation of glycolipid metabolism observed a proliferation of *g_Roseburia* after surgery through the effects of vertical sleeve gastrectomy on bile acids pool and FXR signaling [31]. Other studies demonstrated that *g_Roseburia* was associated with DCA and TCDCA[32,33], aligning with our results. Furthermore, *g_Alloprevotella*, elevated by CSS treatment, showed a negative correlation with lipid indicators (TC, TG, and LDL-C). Previous research suggested that *g_Alloprevotella* was an intestinal probiotic negatively associated with dyslipidemia[34]. Another study also showed a positive correlation between *g_Alloprevotella* and DCA in NAFLD mice with disturbed lipid metabolism[35]. However, the exact relationship of HDCA and CSS significantly regulated bacteria, including *g_norank_Muribaculaceae*, *g_Roseburia*, and *g_Alloprevotella*, with bile acid metabolism and the effect of lipid metabolism regulation needs to be determined by further bacterial intervention experiments.

A notable finding of this research was the significant impact of HDCA and CSS on bile acid metabolism. Consistent with previous studies, CDCA levels were elevated in the HDCA group, likely due to the activation of alternative pathways mediated by CYP7B1[36]. The observed increase in UDCA may result from the action of 7α/β-hydroxysteroid dehydrogenase (7α/β-HSDH) in response to elevated CDCA, where CDCA is first converted to 7-keto-lithocholic acid (7keto-LCA) via 7α-HSDH and subsequently to UDCA via 7β-HSDH[37,38]. Several studies suggested that reducing bile acid synthesis and promoting bile acid excretion could decrease lipid absorption[39,40].

Signaling receptor analysis suggested that HDCA may activate the hepatic FXR and SHP to inhibit downstream CYP7A1 and CYP8B1. Thus, the synthesis of bile acids in the liver was inhibited and the excretion of bile acids was increased, so as to reduce the absorption of lipids (Figure 8**)**. About 95% of the bile acids at the end of the intestines are reabsorbed through the portal vein back to the liver, and it's part of the enterohepatic circulation[7]. After HDCA was administered orally, it was transferred to the liver due to

enterohepatic circulation. The formation of THDCA and GHDCA was achieved through the conjugation of HDCA with taurine and glycine, catalyzed by amino acid N-acyltransferase[37]. Elevated high levels of THDCA and GHDCA in our results may indicate significantly elevated levels of HDCA in the liver.Previous a study also showed that HDCA was significantly enriched after oral administration in liver, where HDCA played a metabolic regulation function[41]. Thus, HDCA may have a more pronounced role in the regulation of hepatic FXR. CSS is a cholesterol sulfation derivative catalyzed by hydroxysteroid sulfotransferases (SULT), which attach a sulfate group to the hydroxyl group of the cholesterol sterol ring in the cytoplasm and the Golgi membrane[42]. Certain gut microbiota encoding SULT, adenosine-5′-phosphosulfate (APS) kinase and enzymes of synthesizing bifunctional 3′-phosphoadenosine 5′-phosphosulfate (PAPS) could also produce CSS, such as *Bacteroides thetaiotaomicron*[43]. CSS has many physiologic functions, such as relieving intestinal inflammation, Regulating glucose and lipid metabolism, and protecting cancer cells from cytotoxic T-cells[44]. Rodents and humans exhibit high levels of CS in both intestinal tissue and feces[44].Our observations indicated that CSS may inhibit hepatic bile acid synthesis to reduce lipid uptake by activating intestinal FXR to elevate FGF15 for inhibiting CYP7A1 and CYP8B1 (Figure 8**)**. FXR activation is dependent on a conformational change in the ligand-binding structural domain (LBD) of the FXR. The hydrophobic steroidal backbone of the CSS binds to hydrophobic residues (ILE335 and PHE461) within the LBD of the FXR. The sulfate group at the 3β position of CSS forms a hydrogen bond with the ARG331 polar residue in FXR-LBD. These two binding modes induce H12 folding thereby exposing the coactivator NcoA binding site and initiating transcriptional activation function[45]. The strong polar sulfate at the 3β position of CSS makes it more hydrophilic, which limits its transmembrane transport behavior in the intestine[46]. Moreover, there is limited expression of organic anion-transporting polypeptide (OATP) that transports CSS in the intestine[47]. CSS may be more difficult to be reabsorbed in the intestine into the portal vein and its main action may be in intestine. Therefore, CSS may tend to modulate intestinal FXR. However, the specific mechanisms still need to be studied in deeper research. Concurrently, LCA and DCA were promoted with CSS intervention. LCA and DCA, as FXR activators, may have an additional role in the activation of intestinal FXR[48]. The bile acid pool was changed may be due to supplementation with HDCA and CSS impacting gut microbiota composition that participated in the production of secondary bile acids[49]. However, the interactions between gut microbiota and bile acids are complex, and dynamic changes in the bile acid pool significantly impact the organism's metabolic functions. Further investigation is warranted to elucidate the mechanisms by which dynamic bile acid pool changes regulate lipid metabolism. In addition, our study lacked functional validation for hepatic or intestinal FXR. Thus, the regulatory mechanisms of HDCA and CSS still need to be further verified via hepatic and intestinal FXR specific knockout mouse experiments, respectively.

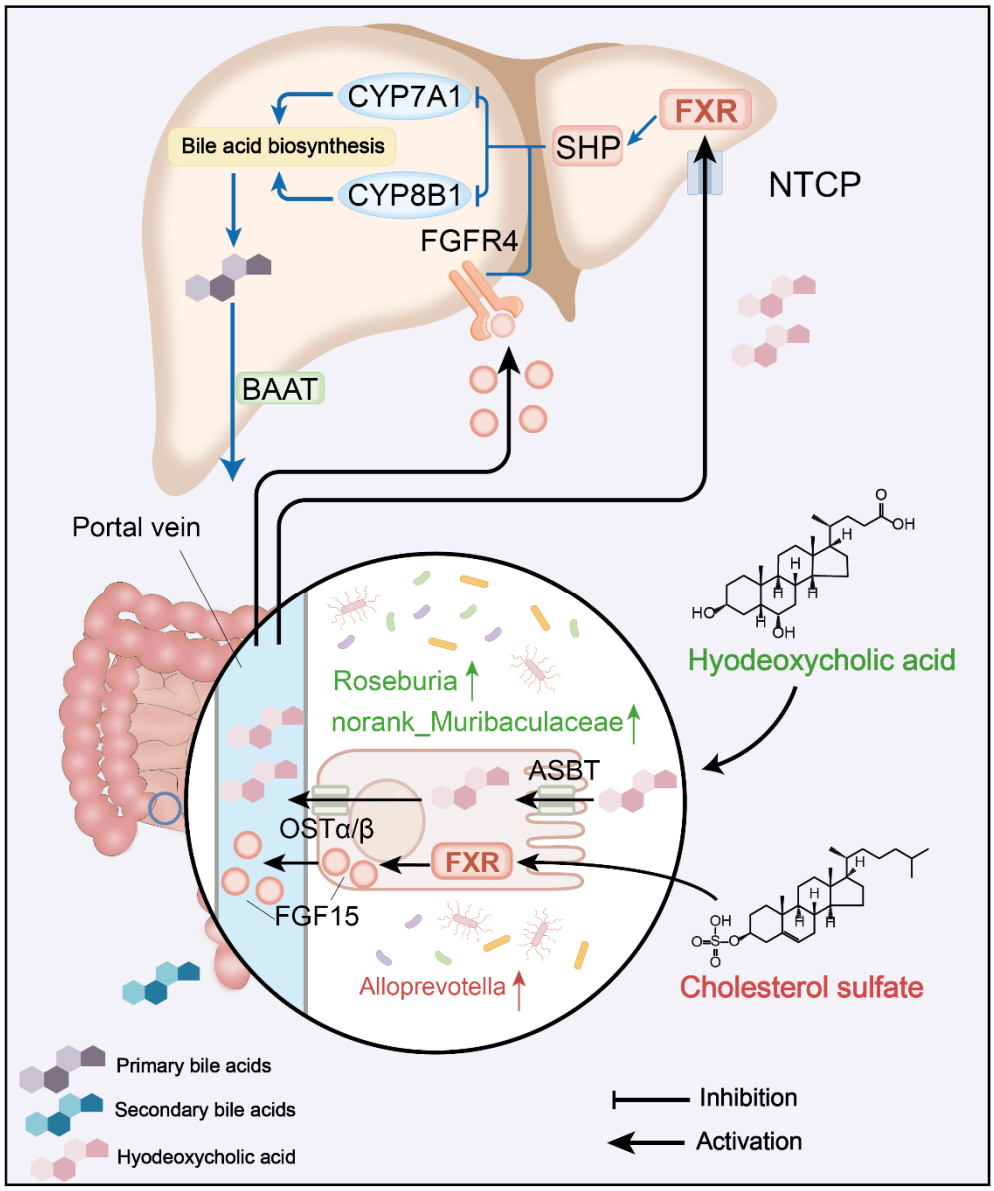

Figure 8. Schematic representation of HDCA and CSS mediated FXR to alleviate lipid metabolism disorders.

5. Conclusion

In conclusion, we aimed to identify bioactive metabolites through the lens of the interplay between the HD pattern and dyslipidemia gut microbiota. We found that intestinal steroid metabolites, HDCA and CSS, could play a role in modulating lipid metabolism, supported by integrative analysis of metabolome in the humanized dyslipidemia mice model, combined with molecular docking and cell culture. Oral administration indicated that HDCA and CSS may modulate bile acid metabolism to improve dyslipidemia via hepatic or intestinal FXR-mediated bile acid synthesis. In addition, the relative abundance of *g_Roseburia* and *g_norank_Muribaculaceae* was elevated by HDCA. Proliferation of *g_Alloprevotella* was promoted by CSS. Furthermore, alterations in bile acid pools were associated with changes in gut microbiota induced by HDCA and CSS. These findings enhanced our understanding of the mechanisms by which intestinal steroid metabolites (HDCA and CSS) regulate host lipid metabolism. Moreover, our study demonstrated that modulating the FXR may be effective way for intestinal steroid metabolites to alleviate

dyslipidemia. Our work found the potential active metabolites HDCA and CSS from the interaction of HD patterns with the gut microbiota, providing new insights into the mechanism of regulating lipid metabolism.

Funding

This study was supported by the Guangxi Science and Technology Base and Talent Special Project (Project No. 2021AC19445) and the National Natural Science Foundation of China (Project No. 32460596).

Notes

The authors declare no competing financial interest.

Acknowledgments

We gratefully acknowledge the Chaozhou Branch of Chemistry and Chemical Engineering Guangdong Laboratory for providing the untargeted metabolome analysis on the feces samples with UPLC-MS/MS. We thank all healthcare staff working in medical examination center of the Fourth People's Hospital of Nanning and Guangxi University Hospital, Guangxi Province, China.

References

[1] D. Li, Y. J. Li, S. J. Yang, et al., Diet-gut microbiota-epigenetics in metabolic diseases: From mechanisms to therapeutics, Biomedicine & Pharmacotherapy 153 (2022) 113290. http://10.1016/j.biopha.2022.113290.

[2] L. N. Xu, Q. Q. Yang, J. H. Zhou, Mechanisms of Abnormal Lipid Metabolism in the Pathogenesis of Disease, International Journal of Molecular Sciences 25 (2024) 8465. http://10.3390/ijms25158465.

[3] Q. Liu, Q. R. Wen, J. Lv, et al., The Prospective Associations of Lipid Metabolism-Related Dietary Patterns with the Risk of Diabetes in Chinese Adults, Nutrients 14 (2022) 980. http://10.3390/nu14050980.

[4] B. K. Perler, E. S. Friedman, G. D. Wu, The Role of the Gut Microbiota in the Relationship Between Diet and Human Health, Annual Review of Physiology 85 (2023) 449-468. http://10.1146/annurev-physiol-031522-092054.

[5] H. Cheng, D. D. Zhang, J. Wu, et al., Interactions between gut microbiota and polyphenols: A mechanistic and metabolomic review, Phytomedicine 119 (2023) 154979. http://10.1016/j.phymed.2023.154979.

[6] X. R. Song, Y. A. Liu, X. Zhang, et al., Role of intestinal probiotics in the modulation of lipid metabolism: implications for therapeutic treatments, Food Science and Human Wellness 12 (2023) 1439-1449. http://10.1016/j.fshw.2023.02.005.

[7] S. L. Collins, J. C. Stine, J. E. Bisanz, et al., Bile acids and the gut microbiota: metabolic interactions and impacts on disease, Nature Reviews Microbiology 21 (2023) 236-247. http://10.1038/s41579-022-00805-x.

[8] Z. L. Cheng, Y. X. Chen, B. Schnabl, et al., Bile acid and nonalcoholic steatohepatitis: Molecular insights and therapeutic targets, Journal of Advanced Research 59 (2024) 173-187. http://10.1016/j.jare.2023.06.009.

[9] Y. T. Xu, C. Y. Zhou, M. Y. Zong, et al., High-protein high-konjac glucomannan diets changed glucose and lipid metabolism by modulating colonic microflora and bile acid profiles in healthy mouse models, Food & Function 15 (2024) 4446-4461. http://10.1039/d4fo00159a.

[10] Z. Song, J. Q. Chen, Y. Ji, et al., Amuc attenuates high-fat diet-induced metabolic disorders linked to the regulation of fatty acid metabolism, bile acid metabolism, and the gut microbiota in mice, International Journal of Biological Macromolecules 242 (2023) 124650. http://10.1016/j.ijbiomac.2023.124650.

[11] J. P. Song, X. Y. Lu, D. H. Liu, et al., Fucogalactan Sulfate (FS) from Laminaria japonica Regulates Lipid Metabolism in Diet-Induced Humanized Dyslipidemia Mice via an Intestinal FXR-FGF19-CYP7A1/CYP8B1 Pathway, Journal of Agricultural and Food Chemistry 71 (2023) 14027-14037. http://10.1021/acs.jafc.3c04683.

[12] C. Xue, P. Zeng, K. Gong, et al., Nogo-B inhibition facilitates cholesterol metabolism to reduce hypercholesterolemia, Cell Reports 43 (2024) 114691. http://10.1016/j.celrep.2024.114691.

[13] S. W. Chen, S. W. Sun, Y. A. Feng, et al., Diosgenin attenuates nonalcoholic hepatic steatosis through the hepatic FXR-SHP-SREBP1C/PPARα/CD36 pathway, European Journal of Pharmacology 952 (2023) 175808. http://10.1016/j.ejphar.2023.175808.

[14] H. T. Xu, F. Fang, K. Z. Wu, et al., Gut microbiota-bile acid crosstalk regulates murine lipid metabolism via the intestinal FXR-FGF19 axis in diet-induced humanized dyslipidemia, Microbiome 11 (2023) 262. http://10.1186/s40168-023-01709-5.

[15] C. Wan, K. Z. Wu, X. Y. Lu, et al., Integrative Analysis of the Gut Microbiota and Metabolome for In Vitro Human Gut Fermentation Modeling, Journal of Agricultural and Food Chemistry 69 (2021) 15414-15424. http://10.1021/acs.jafc.1c04259.

[16] W. Yu, Y. Zhao, Y. Zhang, et al., Gut microbial metabolites-mediated modulation of colitis in mice by three geographically varied dietary patterns, Food Science and Human Wellness (2024). http://10.26599/FSHW.2024.9250420.

[17] K. A. Krautkramer, J. Fan, F. Bäckhed, Gut microbial metabolites as multi-kingdom intermediates, Nature Reviews Microbiology 19 (2021) 77-94. http://10.1038/s41579-020-0438-4.

[18] Z. J. Du, J. Comer, Y. H. Li, Bioinformatics approaches to discovering food-derived bioactive peptides: Reviews and perspectives, Trac-Trends in Analytical Chemistry 162 (2023) 117051. http://10.1016/j.trac.2023.117051.

[19] N. Katsiki, D. P. Mikhailidis, C. S. Mantzoros, Non-alcoholic fatty liver disease and dyslipidemia: An update, Metabolism-Clinical and Experimental 65 (2016) 1109-1123. http://10.1016/j.metabol.2016.05.003.

[20] Y. H. Zhou, J. Y. Zhang, K. Xu, et al., Fucoxanthin improves serum lipids, liver metabolism and gut microbiota in hyperlipidemia mice, Food Science and Human Wellness 14 (2025) 14. http://10.26599/fshw.2024.9250017.

[21] G. Hajjar, M. C. B. Santos, J. Bertrand-Michel, et al., Scaling-up metabolomics: Current state and perspectives, Trac-Trends in Analytical Chemistry 167 (2023) 117225. http://10.1016/j.trac.2023.117225.

[22] K. Wang, M. F. Liao, N. Zhou, et al., Parabacteroides distasonis Alleviates Obesity and Metabolic Dysfunctions via Production of Succinate and Secondary Bile Acids, Cell Reports 26 (2019) 222-235.e5. http://10.1016/j.celrep.2018.12.028.

[23] H. Wang, Y. Guo, W. T. Han, et al., Tauroursodeoxycholic Acid Improves Nonalcoholic Fatty Liver Disease by Regulating Gut Microbiota and Bile Acid Metabolism, Journal of Agricultural and Food Chemistry 72 (2024) 20194-20210. http://10.1021/acs.jafc.4c04630.

[24] J. W. Cai, B. Rimal, C. T. Jiang, et al., Bile acid metabolism and signaling, the microbiota, and metabolic disease, Pharmacology & Therapeutics 237 (2022) 108238. http://10.1016/j.pharmthera.2022.108238.

[25] A. Perino, K. Schoonjans, Metabolic Messengers: bile acids, Nature Metabolism 4 (2022) 416-423. http://10.1038/s42255-022-00559-z.

[26] S. Y. Ke, Recent Progress of Novel Steroid Derivatives and Their Potential Biological Properties, Mini-Reviews in Medicinal Chemistry 18 (2018) 745-775. http://10.2174/1389557517666171003103245.

[27] S. Watanabe, Z. E. Chen, K. Fujita, et al., Hyodeoxycholic Acid (HDCA) Prevents Development of Dextran Sulfate Sodium (DSS)-Induced Colitis in Mice: Possible Role of Synergism between DSS and HDCA in Increasing Fecal Bile Acid Levels, Biological & Pharmaceutical Bulletin 45 (2022) 1503-1509. http://10.1248/bpb.b22-00373.

[28] Y. J. Song, H. T. Shen, T. T. Liu, et al., Effects of three different mannans on obesity and gut microbiota in high-fat diet-fed C57BL/6J mice, Food & Function 12 (2021) 4606-4620. http://10.1039/d0fo03331f.

[29] H. L. Zeng, S. Q. He, Z. X. Xiong, et al., Gut microbiota-metabolic axis insight into the hyperlipidemic effect of lotus seed resistant starch in hyperlipidemic mice, Carbohydrate Polymers 314 (2023) 120939. http://10.1016/j.carbpol.2023.120939.

[30] Q. Q. Feng, Z. T. Niu, S. Q. Zhang, et al., Protective Effects of White Kidney Bean (Phaseolus vulgaris L.) against Diet-Induced Hepatic Steatosis in Mice Are Linked to Modification of Gut Microbiota and Its Metabolites, Nutrients 15 (2023) 3033. http://10.3390/nu15133033.

[31] K. K. Ryan, V. Tremaroli, C. Clemmensen, et al., FXR is a molecular target for the effects of vertical sleeve gastrectomy, Nature 509 (2014) 183-188. http://10.1038/nature13135.

[32] X. P. Li, Y. C. Xiao, L. Q. Song, et al., Effect of Lactobacillus plantarum HT121 on serum lipid profile, gut microbiota, and liver transcriptome and metabolomics in a highcholesterol diet-induced hypercholesterolemia rat model, Nutrition 79-80 (2020) 110966. http://10.1016/j.nut.2020.110966.

[33] H. Lin, Y. P. An, H. R. Tang, et al., Alterations of Bile Acids and Gut Microbiota in Obesity Induced by High Fat Diet in Rat Model, Journal of Agricultural and Food Chemistry 67 (2019) 3624-3632. http://10.1021/acs.jafc.9b00249.

[34] H. Y. Zhou, K. Liu, W. J. Liu, et al., Diets Enriched in Sugar, Refined, or Whole Grain Differentially Influence Plasma Cholesterol Concentrations and Cholesterol Metabolism Pathways with Concurrent Changes in Bile Acid Profile and Gut Microbiota Composition in ApoE-/-Mice, Journal of Agricultural and Food Chemistry 71 (2023) 9738-9752. http://10.1021/acs.jafc.3c00810.

[35] C. Jin, T. T. Zhou, Z. H. Duan, et al., Effect of chin brick tea Camellia sinensis (L.) Kuntze on lipid metabolism and inflammation by modulating intestinal flora and bile acids in mice with non-alcoholic fatty liver disease, Journal of Ethnopharmacology 318 (2024) 116950. http://10.1016/j.jep.2023.116950.

[36] J. L. Kuang, J. Y. Wang, Y. T. Li, et al., Hyodeoxycholic acid alleviates non-alcoholic fatty liver disease through modulating the gut-liver axis, Cell Metabolism 35 (2023) 1752-1766.e8. http://10.1016/j.cmet.2023.07.011.

[37] J. W. Xiang, Z. Y. Zhang, H. Y. Xie, et al., Effect of different bile acids on the intestine through enterohepatic circulation based on FXR, Gut Microbes 13 (2021) 1949095. http://10.1080/19490976.2021.1949095.

[38] P. Lepercq, P. Gérard, F. Béguet, et al., Epimerization of chenodeoxycholic acid to ursodeoxycholic acid by Clostridium baratii isolated from human feces, Fems Microbiology Letters 235 (2004) 65-72. http://10.1016/j.femsle.2004.04.011.

[39] L. Xiao, G. F. Xu, S. L. Chen, et al., Kaempferol ameliorated alcoholic liver disease through inhibiting hepatic bile acid synthesis by targeting intestinal FXR-FGF15 signaling, Phytomedicine 120 (2023) 155055. http://10.1016/j.phymed.2023.155055.

[40] W. Zeng, M. J. Sun, J. M. Cao, et al., Triterpenoids from ilicis rotundae cortex ameliorate hyperlipidemia by affecting bile acids-hepatointestinal FXR axis, Phytomedicine 139 (2025) 17. http://10.1016/j.phymed.2025.156537.

[41] J. Zhong, X. F. He, X. X. Gao, et al., Hyodeoxycholic acid ameliorates nonalcoholic fatty liver disease by inhibiting RAN-mediated PPARa nucleus-cytoplasm shuttling, Nature Communications 14 (2023) 18. http://10.1038/s41467-023-41061-8.

[42] C. A. Strott, Y. Higashi, Cholesterol sulfate in human physiology: what's it all about?, Journal of Lipid Research 44 (2003) 1268-1278. http://10.1194/jlr.R300005-JLR200.

[43] L. N. Yao, G. D. D'Agostino, J. Park, et al., A biosynthetic pathway for the selective sulfonation of steroidal metabolites by human gut bacteria, Nature Microbiology 7 (2022) 1404-+. http://10.1038/s41564-022-01176-y.

[44] X. Q. Yu, S. M. Lei, Y. Shen, et al., Cholesterol Sulfate: Pathophysiological Implications and Potential Therapeutics, Biomolecules 15 (2025) 23. http://10.3390/biom15050646.

[45] L. Y. Jiang, H. J. Zhang, D. S. Xiao, et al., Farnesoid X receptor (FXR): Structures and ligands, Computational and Structural Biotechnology Journal 19 (2021) 2148-2159. http://10.1016/j.csbj.2021.04.029.

[46] L. D. Sanchez, L. Pontini, M. Marinozzi, et al., Cholesterol and oxysterol sulfates: Pathophysiological roles and analytical challenges, British Journal of Pharmacology 178 (2021) 3327-3341. http://10.1111/bph.15227.

[47] J. W. Mueller, L. C. Gilligan, J. Idkowiak, et al., The Regulation of Steroid Action by Sulfation and Desulfation, Endocrine Reviews 36 (2015) 526-563. http://10.1210/er.2015-1036.

[48] S. Li, X. Chen, L. Zhou, et al., Farnesoid X receptor signal is involved in deoxycholic acid-induced intestinal metaplasia of normal human gastric epithelial cells, Oncology Reports 34 (2015) 2674-2682. http://10.3892/or.2015.4207.

[49] B. B. Wang, D. Han, X. Y. Hu, et al., Exploring the role of a novel postbiotic bile acid: Interplay with gut microbiota, modulation of the farnesoid X receptor, and prospects for clinical translation, Microbiological Research 287 (2024) 127865. http://10.1016/j.micres.2024.127865.